TITLE PAGE

The novel anthracenedione, pixantrone, lacks redox activity and inhibits doxorubicinol

formation in human myocardium: Insight to explain the cardiac safety of pixantrone

in doxorubicin treated patients

Emanuela Salvatorelli, Pierantonio Menna, Odalys Gonzalez Paz, Massimo Chello, Elvio Covino,

Jack W. Singer, and Giorgio Minotti

Drug Sciences (E.S., P.M., O.G.P., G.M.) and Cardiac Surgery (M.C., E.C.), Center for Integrated

Research, University Campus Bio-Medico, Rome, Italy

Cell Therapeutics Inc., Seattle, WA (J.W.S.)

1

JPET # 200568

RUNNING TITLE PAGE

RUNNING TITLE: Doxorubicin and the cardiac safety of pixantrone

CORRESPONDING AUTHOR ADDRESS:

Giorgio Minotti

CIR and Drug Sciences

University Campus Bio-Medico

Via Alvaro del Portillo, 21

00128 Rome - ITALY

TELEPHONE: 011-39-06-225419109

FAX: 011-39-06-22541456

E-MAIL: g.minotti@unicampus.it

NUMBER OF TEXT PAGES : 21

NUMBERS OF TABLES : 3

NUMBER OF FIGURES : 9

NUMBER OF REFERENCES : 59

NUMBER OF WORDS   Abstract : 247

Introduction: 718

Discussion : 1498

NONSTANDARD ABBREVIATIONS : DOX, doxorubicin; CHF, congestive heart failure; C_{max}, peak concentration; $O_2^{\cdot-}$, superoxide anion; H_2O_2, hydrogen peroxide; ROS, reactive oxygen species; DOXOL, doxorubicinol; DLBCL, diffuse large B-cell lymphoma; MITOX, mitoxantrone; PIX, pixantrone; NHL, non-Hodgkin's lymphoma; CHOP, cyclophosphamide/DOX/vincristine/prednisone; DCFH-DA, dichlorofluorescin-diacetate; DCF, dichlorofluorescein; HPLC, high performance liquid chromatography; HRP, horseradish peroxidase; LC-MS, liquid chromatography-mass spectrometry; ESI(+)/MRM, electron spray ionization(+)/multiple reaction monitoring; SIM, single ion monitoring; MDR, multidrug resistance; MRP1, Multidrug Resistance Protein 1; IC_{50}, half maximal inhibitory concentration.

ABSTRACT

Cardiotoxicity from the antitumor anthracycline, doxorubicin, correlates with doxorubicin cardiac levels, redox activation to superoxide anion ($O_2^{\cdot-}$) and hydrogen peroxide (H_2O_2), formation of the long-lived secondary alcohol metabolite, doxorubicinol. Cardiotoxicity may first manifest during salvage therapy with other drugs, such as the anthracenedione mitoxantrone. Minimal evidence for cardiotoxicity in anthracycline-pretreated patients with refractory-relapsed non Hodgkin's lymphoma was observed with the novel anthracenedione, pixantrone. We characterized whether pixantrone and mitoxantrone caused different effects on doxorubicin levels, redox activation, doxorubicinol formation. Pixantrone and mitoxantrone were probed in a validated ex vivo human myocardial strip model that was either doxorubicin-naïve or preliminarily subjected to doxorubicin loading and washouts to mimic doxorubicin treatment and elimination in the clinical setting. In doxorubicin-naïve strips, pixantrone showed higher uptake than mitoxantrone; however, neither drug formed $O_2^{\cdot-}$ or H_2O_2. In doxorubicin-pretreated strips, pixantrone or mitoxantrone did not alter the distribution and clearance of residual doxorubicin. Mitoxantrone showed an unchanged uptake, lacked effects on doxorubicin levels, but synergized with doxorubicin to form more $O_2^{\cdot-}$ and H_2O_2, as evidenced by $O_2^{\cdot-}$-dependent inactivation of mitochondrial aconitase or mitoxantrone oxidation by H_2O_2-activated peroxidases. In contrast, pixantrone uptake was reduced by prior doxorubicin exposure; moreover, pixantrone lacked redox synergism with doxorubicin, and formed an N-dealkylated product that inhibited metabolism of residual doxorubicin to doxorubicinol. Redox inactivity and inhibition of doxorubicinol formation correlate with the cardiac safety of pixantrone in doxorubicin-pretreated patients. Redox inactivity in the face of high cardiac uptake suggests that pixantrone might be safe also in doxorubicin-naïve patients.

INTRODUCTION

Clinical use of doxorubicin (DOX) and other topoisomerase II-inhibiting antitumor anthracyclines is limited by dose-related cardiotoxicity. In adults, cumulative doses of 400-450 mg/m^2 of DOX introduce a 5% risk of congestive heart failure (CHF) (Swain et al., 2003). In children, even lower cumulative doses introduce a lifetime risk of cardiotoxicity (Barry et., 2007).

Anthracycline cardiotoxicity is a multifactorial and incompletely defined process, but a few basic determinants have been identified. Cardiotoxicity correlates with the plasma C_{max} of DOX and its accumulation in the heart, which depends on the balance between DOX uptake and clearance (Minotti et al., 2004). Clearance seems to be incomplete, as DOX can be found in the hearts of patients expiring months or years after the last administration (Stewart et al., 1993). Moreover, the risk of cardiotoxicity increases significantly if DOX undergoes reductive bioactivation. DOX is composed of a tetracyclic quinone-hydroquinone chromophore, an aminosugar, and a short side chain with a carbonyl group (**Figure 1**). One-electron reduction of the quinone yields a semiquinone that reduces oxygen to superoxide anion ($O_2^{\cdot-}$) and its dismutation product, hydrogen peroxide (H_2O_2), members of the broad family of reactive oxygen species (ROS) that cause oxidative stress in the relatively unprotected heart (Doroshow, 1983; Gewirtz, 1999). Two-electron reduction of the side chain carbonyl moiety generates a secondary alcohol metabolite (doxorubicinol, DOXOL, Figure 1). Being more polar than DOX, DOXOL shows essentially no cardiac clearance (Salvatorelli et al., 2007). DOXOL accumulation exposes the heart to a lifetime risk of CHF (Blanco et al., 2012; Minotti et al., 2010).

Cardiotoxicity also complicates the clinical management of patients who progress or relapse after first line therapy with ≤400 mg/m^2 of DOX. Second or third line non-anthracycline chemotherapeutics might precipitate cardiotoxicity by interfering with the cardiac clearance of DOX or by forming ROS or by increasing DOXOL formation. The risk of cardiotoxicity may be higher when salvage drugs share structural or functional similarities with DOX (Minotti et al., 2004).

Anthracenediones are aglyconic quinone-hydroquinone drugs with anthracycline-like antitumor activity. Although traditionally grouped with anthracyclines, anthracenediones show

4

important structural differences: the chromophore contains three rings only, and the side chains lack carbonyl groups precursor of secondary alcohol metabolites. In patients with diffuse large B-cell lymphoma (DLBCL), the prototypic anthracenedione, mitoxantrone (MITOX) (Figure 1), was less efficacious than DOX, but had similar cardiotoxicity (Osby et al., 2003; Sonneveld et al., 1995). MITOX exacerbates cardiotoxicity in anthracycline-pretreated laboratory animals (Cavalletti et al., 2007) and patients (Faulds et al., 1991).

Pixantrone (PIX) is a novel anthracenedione that differs from MITOX due to removal of the hydroquinone, insertion of a nitrogen heteroatom in the same ring, and substitution of (ethylamino)-diethylamino for (hydroxyethylamino)-ethylamino side chains (Figure 1). PIX caused essentially no cardiotoxicity in anthracycline- naïve or -pretreated animals (Cavalletti et al., 2007). In phase I studies, PIX was tolerable at doses associated with antitumor activity, and this activity was pronounced in patients with late-stage refractory/relapsed aggressive non-Hodgkin's lymphoma (NHL) (Borchmann et al., 2001). Therefore, PIX was developed to treat patients with NHL who progress or relapse after DOX-containing chemotherapy regimens. In the phase III EXTEND study of patients with NHL who had received the cyclophosphamide/DOX/vincristine/prednisone regimen (CHOP) with a median cumulative dose of ~300 mg/m^2 of DOX, single-agent PIX was tolerable and demonstrated a significantly higher complete response rate and progression free survival than investigator's choice of single-agent chemotherapeutics (Pettengell et al., 2012). Rapidly reversible grade 3 reductions in left ventricular ejection fraction were observed in 2 of 68 (3%) PIX-treated patients. The study resulted in conditional approval by the European Medicines Agency for PIX as monotherapy in patients with relapsed aggressive B-cell NHL who are not candidates for stem cell transplantation.

Studies of cardiac safety or toxicity of antitumor drugs are limited by differences in drug metabolism between humans and laboratory animals (Menna et al., 2008; Minotti et al., 2004; Mordente et al., 2003). We validated an *ex vivo* human myocardial strip model that eliminated this problem and helped to characterize DOX accumulation and bioactivation to ROS or DOXOL in human myocardium (Salvatorelli, Guarnieri et al., 2006; Salvatorelli, Menna et al., 2006; Salvatorelli et al., 2007; Salvatorelli et al., 2009; Salvatorelli et al., 2012a; Salvatorelli et al.,

5

2012b). Here, the same model was used to explore the determinants of PIX cardiac safety in

anthracycline-pretreated patients. MITOX was used as a comparator.

MATERIALS AND METHODS

Chemicals

DOX and DOXOL were obtained from Nerviano Medical Sciences (Milan, Italy). PIX dimaleate and its metabolites were provided by Cell Therapeutics, Inc. (Seattle, WA). Dichlorofluorescin-diacetate (DCFH-DA) and dichlorofluorescein (DCF) were obtained from Invitrogen (Carlsbad, CA). MITOX, verapamil, and all other chemicals, were obtained from Sigma-Aldrich (Milan, Italy).

Human Myocardial Strip Preparation and Incubation with Drugs

One hundred seventy-four myocardial samples were obtained from 126 male patients (69 ± 1.3 yr of age) and 48 female patients (71 ± 2.7 yr) undergoing aortocoronary bypass grafting. All samples were to be routinely disposed of by the surgeons during cannulation of nonischemic, beating right atrium; therefore, the patients were not subjected to any unjustified loss of tissue (Salvatorelli et al., 2012a; Salvatorelli et al., 2012b). Thin strips ($\sim$10 mm long, $\sim$2 mm wide) were dissected free of fat or grossly visible foreign tissues. The strips were incubated in 2 ml of fresh human plasma to allow for effects of binding of drugs to albumin and other proteins (Whitaker et al., 2008). DOX was used at a final concentration of 10 µM, similar to the plasma C_{max} produced by standard DOX infusions (Gianni et al., 1997). PIX was used at 1 µM (calculated as PIX base), similar to the plasma C_{max} produced by 1h infusion of 85 mg/m^2 of PIX in the EXTEND study (Cell Therapeutics Inc, 2010). MITOX was used at 1 µM, which is similar to the plasma C_{max} produced by 14 mg/m^2 of MITOX (Canal et al., 1993), the dose level adopted for MITOX as a comparator to PIX in the EXTEND study (Pettengell et al., 2012).

Probing PIX or MITOX as Single-Agents or in Sequence with DOX

Incubations were carried out at 37°C in a gently shaking Dubnoff metabolic bath under a room air atmosphere. Unless otherwise indicated, four sets of 4 h incubations were performed. In the first experiment, the myocardial strips were incubated with plasma for 2.5 h. Single-agent anthracenedione was then added at 1 µM, and incubation continued for an additional 1.5 h (**Figure 2A**, caption a). In the other three experiments, PIX or MITOX was added in sequence with DOX. In

7

the first condition, DOX was added and allowed to stay over the 4 h length of incubations; anthracenedione was added at 2.5 h (**Figure 2A**, caption b). This condition (*DOX loading*) probed PIX or MITOX in strips subjected to a continuous uptake and retention of DOX. In the second condition, the strips were exposed to DOX for 30 min and then placed in fresh anthracycline-free plasma; after 2.5 h, anthracenedione was added (**Figure 2A**, caption c). This condition (*DOX loading and washout*) probed PIX or MITOX in strips subjected to DOX uptake and clearance. In the third condition, the strips were exposed to DOX for 30 min and then placed in fresh anthracycline-free plasma that was renewed every 30-60 min up to 2.5 h; next, anthracenedione was added (**Figure 2A**, caption d). This condition (*DOX loading and multiple washouts*) probed PIX and MITOX in strips subjected to DOX uptake and more extensive clearance.

<u>Drug Uptake, Clearance, and Accumulation</u>

DOX accumulation was determined by the net levels of DOX retention in the strips at the end of 4 h incubations. In DOX loading/washout(s) experiments, uptake was determined as [(DOX accumulation) + (DOX efflux in plasma)]; DOX clearance was determined as [100 x (efflux/uptake)] (Salvatorelli et al., 2012a). Similar procedures were adopted in *ad hoc* experiments with single-agent anthracenedione. Where indicated, the experimental conditions were modified to measure PIX uptake, clearance, and accumulation, in strips that released increasing levels DOX in plasma. The strips were subjected to 30 min loading with DOX at 1 or 10 μM; next, plasma was replaced fresh, and PIX was added at 1 μM to measure its uptake while DOX diffused from strips in plasma. After 30 more min, plasma was replaced fresh and the incubations were allowed to proceed to measure PIX clearance while also DOX was diffusing from strips in plasma. Strips loaded with only PIX were used as controls.

<u>HPLC assays for DOX and anthracenediones</u>

After incubation, the strips were washed with ice-cold 0.3 M NaCl, homogenized in 1 ml of the same medium, and centrifuged for 90 min at 105,000g to separate soluble and whole-membrane fractions. These were extracted with an equal volume of (90:10) CH_3OH-CH_3CN, acidified with 0.2% CF_3COOH. Plasma was extracted in a similar manner. After centrifugation at 25,000g for 10 min, 100 μl of the supernatant was analyzed by high performance liquid

8

chromatography (HPLC) in a Hewlett-Packard 1100 system (Palo Alto, CA).

We used a (5 μm, 250 x 2.1 mm) Supelcosil™ ABZ+Plus column (Supelco, Bellafonte, USA). The column was operated at 25 °C and eluted at the flow rate of 0.6 ml/min for a total 30 min run time [8 min linear gradient from 100% 50 mM NaH_2PO_4, pH 3.0, to (80%-20%) 50 mM NaH_2PO_4-CH_3CN, followed by a 7 min linear gradient to (65%-35%) 50 mM NaH_2PO_4-CH_3CN, which eventually was switched to a 15 min linear gradient to (50%-50%) 50 mM NaH_2P-CH_3CN]. DOX and DOXOL were detected fluorimetrically (excitation at 480 nm/emission at 560 nm) and identified by co-chromatography with authentic standards. Because of differences in the fluorescence yield of one anthracycline versus another, and of parent anthracyclines versus secondary alcohol metabolites, we did not use an internal standard like e.g., daunorubicin; instead, DOX and DOXOL were quantified against standard curves prepared on the day of the experiment (Salvatorelli et al., 2007). Retention times were 15.0 min for DOX and 13.6 min for DOXOL, with a lowest detection limit of 0.001 μM. PIX and MITOX were detected by diode array spectroscopy (λ_{max} = 642 nm or 610 nm, respectively), identified by co-chromatography with authentic standards, and quantified against appropriate standard curves. Retention times were 6.4 min for PIX and 10.7 min for MITOX; the lowest detection limit was 0.005 μM for PIX or 0.001 μM for MITOX. Extraction efficiency and HPLC recovery always averaged >90%. Within-day and between-days coefficients of variation were ~3 and ~10%, respectively. All values were normalized to tissue weight and expressed as micromolar equivalents since the density of cardiac tissue is very similar to that of water (Mushlin et al., 1993).

HPLC Assay for DCF-Detectable H_2O_2

Basal or drug-stimulated ROS formation was measured by an HPLC adaptation of the method based on the uptake of membrane-permeable DCFH-DA, its intracellular deacetylation to membrane-impermeable DCFH, oxidation of DCFH to DCF by H_2O_2 (Salvatorelli, Guarnieri et al., 2006; Salvatorelli et al., 2007; Salvatorelli et al., 2012b).

Myocardial strips were incubated in 4 ml of 50 mM phosphate buffer/123 mM NaCl/5.6 mM glucose, pH 7.4, to which DCFH-DA was added at 50 μM. After 1 h in the dark, the strips were washed with 0.3 M NaCl and incubated with plasma with or without drugs. In experiments of DOX

9

loading and multiple washouts, the last washout was followed by 30 min re-exposure of the strips to 50 µM DCFH-DA; this was done to compensate for any DCFH-DA that had diffused from strips in plasma during washouts. At the end of the experiment, the strips were homogenized in 2 ml of ice-cold 123 mM NaCl, to which the antioxidant 4-hydroxytempo was added at 1 mM to prevent further oxidation of DCFH to DCF during tissue homogenization. Soluble and membrane fractions were extracted and analyzed by HPLC as described for DOX(OL) and PIX or MITOX, except that the loading volume was 25 µl and the total run time was 25 min [10-min linear gradient from 100% 50 mM NaH_2PO_4, pH 3.0, to (30%-70%) 50 mM NaH_2PO_4-CH_3CN]. The fluorescent peak of DCF (excitation at 488 nm/emission at 525 nm) was identified by co-chromatography with an authentic standard (retention time = 14.0 min) and quantified against a proper standard curve (lowest detection limit = 0.001 µM).

Measurements of ROS by fluorescent probes suffer from potential limitations and artifacts (Kalyanaraman et al., 2012); therefore, the DCF assay adopted in this study had been validated to obtain unambiguous identification of DCF as a marker of H_2O_2-dependent DCFH oxidation, and to establish quantitative correlations between DCF and H_2O_2. Unambiguous identification of DCF as the product of H_2O_2-dependent DCFH oxidation was obtained by measuring, respectively, ∼4-fold or ∼2.5-fold elevations of DCF in strips incubated for 4 h in plasma added with 100 µM antimycin A (which induces a mitochondrial leakage of H_2O_2 by inhibiting complex III in respiratory chain) or 50 mM aminotriazole (which reduces H_2O_2 decomposition by inhibiting catalase) (Salvatorelli, Guarnieri, et al., 2006). Quantitative correlations between DCF and H_2O_2 were obtained by measuring DCF in strips incubated for 15 min in 4 ml of 50 mM phosphate buffer/123 mM NaCl/5.6 mM glucose, pH 7.4, to which H_2O_2 was added at 0.1 to 10 µM. DCF formation in these strips was plotted against a DCF standard curve, and a DCF:H_2O_2 stoichiometry of 0.43 could be established (Salvatorelli, Guarnieri, et al., 2006; Salvatorelli et al., 2012b). The lack of a 1:1 stoichiometry could be attributed to H_2O_2-independent oxidation of DCFH or side reactions of DCF with redox active cell constituents (Rota et al., 1999).

In Vitro Oxidation of PIX or MITOX

Incubations contained 10 μM anthracenedione and 0.01 μM horseradish peroxidase (HRP) in 10 mM ammonium acetate, pH 7.0, 37°C. Oxidation was started by 100 μM H_2O_2 and was terminated after 30 min by inhibiting HRP with 0.5 mM methimazole (Reszka et al., 2011).

LC-MS Analyses of PIX or MITOX Metabolites

PIX metabolites were analyzed by liquid chromatography-mass spectrometry (LC-MS) (Agilent 1200 HPLC-6410 triple quadrupole spectrometer). Cell-free reaction mixtures were injected unmodified; incubations of myocardial strips were extracted as described previously.

We used a (3.5 μm, 100 x 2.1 mm) Eclipse Plus C18 column (Agilent Technologies, Santa Clara, CA). The autosampler was set at 4°C, and the loading volume was 8 μl. For PIX metabolite characterizations, the samples were eluted at a flow rate of 200 μl/min with a mobile phase composed of (90:10) (H_2O-0.1% HCOOH:CH_3CN-0.1% HCOOH), which was changed to (15:85) in 8 min and returned to (90:10) in 5 min. Measurements were done at 350 °C source temperature. CT-45886, CT-45889, CT-45890, and the internal standard (ethopropazine) were detected by electron spray ionization(+)/multiple reaction monitoring (ESI(+)/MRM). The following single charged precursor-product ions were used as quantifier transitions : 283.3-179 m/z (81 eV collision energy) for CT- 45886, 324.3-163.7 m/z (113 eV collision energy) for CT-45889, 324.3-140 m/z (93 eV collision energy) for CT-45890, 314-114.2 m/z (16 eV collision energy) for the internal standard (ethopropazine). Qualifier transitions were: 283.3-265 m/z (1 eV collision energy) for CT-45886, 324.3-277.1 m/z (33 eV collision energy) for CT-45889, 324.3-292.1 m/z (25 eV collision energy) for CT-45890, 314-199.1 m/z (32 eV collision energy) for the internal standard. Drying and nebulizer gases were operated at 11 l/min and 25 psi, respectively; the fragmentor was set at 103 V for CT-45886 or CT-45890, at 152 V for CT-45889, at 123 V for internal standard. The capillary voltage was $4*10^3$ V. To quantify PIX metabolites that diffused from strips in plasma, (ESI(+)/MRM) signals in plasma samples from complete incubations (PIX + strips) were corrected for background signals in plasma samples incubated with PIX only (10% for CT-45886, 13% for CT-45889, 33% for CT-45890).

MITOX metabolite standards were not available; therefore, qualitative assessment of MITOX metabolism was obtained by ESI(+)/single ion monitoring (SIM) of molecular masses that

11

fit in published metabolic modellings (Blanz et al., 1991; Reszka et al., 1997). The samples were eluted at a flow rate of 200 µl/min with a mobile phase composed of (90:10) (H_2O-0.1% HCOOH:CH_3CN-0.1% HCOOH), which was changed to (20:80) in 5 min, maintained isocratic for 3.5 min, and returned to (90:10) in 1.5 min. Single runs of ESI(+)/SIM were performed with the fragmentor at 141 V. In complete incubations (MITOX + strips), ESI(+)/SIM signals were detected only in plasma, which indicated complete diffusion of MITOX metabolites from strips in plasma. Control experiments showed that plasma incubated with only MITOX did not develop ESI(+)/SIM signals.

<u>Mitochondrial Aconitase Assay</u>

Mitochondrial aconitase activity was measured spectrophotometrically by *cis*-aconitate consumption (Minotti, Recalcati, et al., 2004). To improve the assay sensitivity, 105,000g pellets of strip homogenates were resuspended in 0.3 M NaCl and centrifuged at low speed to obtain a supernatant that was partially enriched in mitochondria; moreover, membranes were preincubated for 5 min with cysteine and ferrous ammonium sulfate to obtain maximal reconstitution of the catalytic [4Fe-4S] cluster of aconitase (Minotti, Recalcati, et al., 2004).

<u>Other Conditions</u>

DOX metabolism was characterized in isolated soluble fractions of myocardial strips as reported previously (Salvatorelli et al., 2012b). Proteins were measured by bicinchoninic acid (Stoscheck, 1990). Cardiac troponin I (cTnI) was measured immunoenzymatically (Siemens Medical Diagnostics), and cTnI release was expressed as [100 x (cTnI in plasma)/(cTnI in plasma + cTnI in the strips)] (Salvatorelli et al., 2012b).

<u>Statistical analyses</u>

All values were means $\pm$ standard error (SE) of at least three replicates. Data were analyzed by unpaired Student's t test or one-way ANOVA followed by Bonferroni's test for multiple comparisons; differences were considered significant when *P* was <0.05.

RESULTS

PIX or MITOX Levels in DOX-Loaded Human Myocardial Strips

In human myocardial strips, single-agent PIX accumulated at concentrations ~three times those of MITOX (**Figure 2B**, caption a). DOX loading did not affect PIX accumulation (**Figure 2B**, caption b); however, DOX loading/washout or DOX loading/multiple washouts diminished PIX accumulation by 25% or 45%, respectively (**Figure 2B**, captions c-d). This was not observed with MITOX; it follows that after DOX loading and multiple washouts, PIX accumulated only 1.5 times more than MITOX (see also Figure 2B, captions d). DOX loading/washout and DOX loading/multiple washouts diminished PIX accumulation in both membrane and soluble fractions of the strips; again, this did not occur with MITOX (**Figure 2/C-D**).

Single or multiple washouts induced, respectively, ~40% or ~60% clearance of DOX from myocardial strips, and diminished DOX accumulation in both membrane fraction and soluble fractions of the strips. PIX and MITOX did not affect DOX accumulation, distribution, and clearance (**Table 1**).

In human myocardial strips, many anthracycline-related effects occur over a narrow range of anthracycline levels (Salvatorelli et al., 2006; Salvatorelli et al., 2012a; Salvatorelli et al., 2012b). Inasmuch as single or multiple washouts diminished both the accumulation of DOX and that of PIX added after DOX, we considered that PIX accumulation was limited by the presence of a critical amount of DOX in the strips. This proved not to be case. In DOX loading experiments, decreasing DOX concentration from 10 to 3 µM caused ~66% decrease of DOX accumulation in the strips, which was similar to the decrease induced by multiple washouts in experiments with DOX at 10 µM; however, PIX accumulation was not diminished in comparison with strips exposed to PIX as single agent (not shown). We concluded that PIX accumulation was independent of the net levels of DOX in the strips. By considering that DOX loading experiments probed DOX uptake and retention but not DOX clearance, we also hypothesized that PIX accumulation was limited by effects that only occurred when washouts caused DOX clearance.

13

Single-agent PIX showed higher uptake and clearance than MITOX. PIX uptake was 2.8-fold higher, while clearance was only ~30% higher, indicating that greater accumulation of single-agent PIX was mainly driven by higher uptake (**Table 2**). We next characterized whether DOX clearance interfered with PIX uptake and/or augmented PIX clearance. To obtain this information, we measured PIX uptake and clearance in strips that released increasing amounts of DOX following exposure to the anthracycline at 1 or 10 μM (cfr. Materials and Methods). Under such defined conditions, PIX accumulation was limited by a selective decrease of PIX uptake (**Figure 3/A-C**). Strips exposed to 1 or 10 μM DOX exhibited one order of magnitude difference in the net values of DOX efflux (not shown); nevertheless, both strips caused comparable decreases in PIX uptake and accumulation. This suggested that even minor fluxes of DOX clearance impair PIX uptake.

Mammalian cardiomyocytes constitutively express Multidrug Resistance (MDR) proteins such as Multidrug Resistance Protein 1 (MRP1) (Flens et al., 1996) and P-glycoprotein (Budde et al., 2011), the latter being highly expressed also in endothelial cells (Meissner et al, 2004). We characterized whether in the strips subjected to DOX loading and washouts, MDR proteins extruded PIX and diminished its accumulation. The calcium channel blocker, verapamil, was used to inhibit P-glycoprotein and MRP1 (Vellonen et al., 2004). To avoid confounding effects due to calcium channel blockade, verapamil was used at a concentration level (1 μM) that was high enough to inhibit DOX extrusion by MDR proteins (Salvatorelli et al., 2012a) but was lower than verapamil plasma levels associated with calcium channel blockade and cardiovascular effects in clinical studies of tumor resistance reversal (Motzer et al., 1995; Warner et al., 1998). In the strips sequentially exposed to DOX loading/multiple washouts and PIX, 1 μM verapamil increased the accumulation of DOX but not of PIX (**Figure 3D**).

H_2O_2 Formation by PIX or MITOX in Human Myocardial Strips

In control strips, DCF-detectable H_2O_2 averaged 0.21 ± 0.01 μM. In the light of the low antioxidant defenses of the heart, this value compared reasonably well with the upper limit of the physiologic range of H_2O_2 concentrations measured by other investigators in different cells and tissues (Chance et al., 1979). DOX loading increased H_2O_2 levels by ~70%, while strips subjected

to DOX loading/multiple washouts showed no such increases. PIX or MITOX, as single agents or in sequence with DOX, did not increase DCF-detectable H_2O_2 (**Table 3**).

Correlations of H_2O_2 Formation with Peroxidatic PIX Metabolism

H_2O_2-activated peroxidases contribute to oxidizing DCFH to DCF (LeBel et al., 1992); however, they may also oxidize anthracenediones (Blanz et al., 1991; Reszka et al., 1997). We characterized whether anthracenediones produced H_2O_2 undetected by the DCF assay because of utilization in peroxidatic drug metabolism rather than DCFH oxidation.

In cell-free systems, incubations of PIX with resting HRP caused modifications of PIX side chains, resulting in formation of an N-dealkylated metabolite (CT-45886) and of two N-cyclized metabolites (CT-45889, CT-45890). The relative abundances were 9% for CT-45886 and ≤0.5 % for CT-45889 and CT-45890. Upon activating HRP with H_2O_2, CT-45886 formation remained unchanged while the abundances of CT-45889 or CT-45890 increased to 1.2% and 0.8%, respectively. These results showed that CT-45886 formed by spontaneous hydrolysis of PIX, while CT-45889 and CT-45890 formed both spontaneously and by peroxidatic metabolism.

We next measured PIX metabolites in strips incubated with PIX alone or in sequence with DOX. High levels of CT-45886, the nonperoxidatic metabolite, were recovered from all incubations examined. By measuring CT-45886 in plasma also, we determined that its clearance averaged 59±20%, 31±12%, and 35±12%, in strips exposed to PIX alone or PIX in sequence with DOX loading or DOX loading/multiple washouts, respectively. Total levels of CT-45886 diminished when PIX was added after DOX loading/multiple washouts, which is consistent with the limited accumulation of PIX in these strips (**Figure 4**). CT-45889 and CT-45890, the potentially peroxidatic metabolites, formed in much lower amounts and showed near-to-complete clearance from the strips (93±7% or 94±6%, respectively). Comparable levels of CT-45889 and CT-45890 were measured in experiments with PIX alone or in sequence with DOX loading, which is not consistent with the fact that DOX loading caused H_2O_2 formation in the strips. Neither CT-45889 nor CT-45890 was recovered when PIX was added after DOX loading/multiple washouts, which is consistent with the limited accumulation of PIX in these strips (Figure 4). These results suggested that the levels of potentially peroxidatic metabolites correlated poorly with H_2O_2 formation; such

15

metabolites probably formed by spontaneous rearrangements that did not consume H_2O_2 in competition with the DCF assay. We confirmed that PIX did not form H_2O_2 in the strips.

<u>Correlations of H_2O_2 Formation with Peroxidatic MITOX Metabolism</u>

In cell-free experiments, MITOX converted to metabolites only after HRP had been activated with H_2O_2 (not shown). Single-agent MITOX was also stable in the strips, but six putative metabolites were identified when MITOX was used in sequence with DOX loading; two of these metabolites also formed when MITOX was used in sequence with DOX loading/multiple washouts. All metabolites diffused completely from strips in plasma.

MITOX metabolites showed different patterns of oxidation. In strips with high DOX levels (DOX loading), MITOX converted to both strongly and mildly oxidized metabolites that exhibited combinations of hydroquinone oxidation with side chain N-cyclization or C-terminus peroxidation or carboxylation. In strips with low DOX levels (DOX loading/multiple washouts), MITOX converted to mildly oxidized metabolites that exhibited only hydroquinone oxidation or side chain N-cyclization or C-terminus carboxylation (**Figure 5**). Two strongly oxidized metabolites (A and C in Figure 5) were the same as those identified in cell-free experiments. These results suggested that in the presence of low to high DOX levels, increasing amounts of H_2O_2 were consumed to oxidize MITOX rather than DCFH. We concluded that MITOX synergized with DOX in increasing H_2O_2 formation.

<u>Metabolism-related Refinements of Anthracenedione Accumulation</u>

We examined whether the values of anthracenedione accumulation required corrections that incorporated formation and clearance of metabolites. No correction was required for the values determined in loading/washout experiments with single-agent anthracenedione: loading was too brief for PIX to generate its most abundant and least diffusible metabolite, CT-45886, and MITOX did not form metabolites. In 4 h experiments of anthracenediones as single agents or in sequence with DOX, no correction was required for MITOX accumulation, as MITOX metabolites diffused completely. With PIX, a *theoretical* accumulation was calculated to correct for partial retention of CT-45886. Theoretical accumulation (PIX + CT-45886) was significantly higher than *apparent* accumulation determined by measuring PIX only. Theoretical accumulation was diminished in the

strips subjected to DOX loading/multiple washouts, but remained >3 times higher than MITOX accumulation (**Figure 6**).

cTnI Release or Mitochondrial Aconitase Inactivation by PIX or MITOX

DOX and/or anthracenediones did not induce myocardial release of cTnI, marker of acute stress and necrosis. A sizeable release of cTnI only occurred when the strips were exposed to a bolus of 100 µM H_2O_2 (**Figure 7/A-B**). We characterized whether DOX and/or anthracenediones induced subthreshold damage by inactivating mitochondrial aconitase, whose catalytic [4Fe-4S] cluster decays upon exposure to ROS and in particular to $O_2^{\cdot-}$, precursor of H_2O_2. Superoxide anion is, in fact, much more reactive than H_2O_2 toward aconitase (estimated rate constants of ~10^7 M^{-1} s^{-1} and ~10^2 M^{-1} s^{-1}, respectively). This makes mitochondrial aconitase inactivation an exquisite marker of formation of pathophysiologic amounts of $O_2^{\cdot-}$ in cells and tissues (Gardner, 2002; Salvatorelli, Guarnieri et al., 2006; Salvatorelli et al., 2012b). Monitoring $O_2^{\cdot-}$ formation by aconitase inactivation could also be used for correlations with, and validation of H_2O_2 measurements by the DCF assay.

Mitochondrial aconitase was inactivated after DOX loading but not after DOX loading/multiple washouts, which correlated well with H_2O_2 being increased after DOX loading but not after DOX loading/multiple washouts (cfr. Table 3). MITOX alone did not inactivate mitochondrial aconitase; however, MITOX increased aconitase inactivation induced by DOX loading and also caused aconitase inactivation in strips subjected to DOX loading/multiple washouts (**Figure 7C**). PIX alone did not inactivate mitochondrial aconitase, did not increase aconitase inactivation from DOX loading, and did not cause aconitase inactivation in strips subjected to DOX loading/multiple washouts (**Figure 7D**). These results confirmed that PIX lacks activity in ROS formation, while MITOX synergizes with DOX in causing more $O_2^{\cdot-}$ formation.

Effects of PIX or MITOX on DOXOL Formation

DOX is metabolized to DOXOL by NADPH-dependent cytoplasmic reductases (Blanco et al., 2012; Kalabus et al., 2012; Menna et al., 2008; Minotti et al., 2004; Mordente et al., 2003; Slupe et al., 2005). In the soluble fraction of strips incubated with DOX, DOXOL formation

increased with DOX levels in the following order: DOX loading/multiple washouts < DOX loading/washout < DOX loading (**Figure 8A**). Anthracenediones did not affect DOXOL levels after DOX loading or DOX loading/washout. In the strips subjected to DOX loading/multiple washouts, DOXOL levels were significantly diminished by PIX but not by MITOX (**Figure 8B**).

PIX did not induce DOXOL efflux from strips (not shown); therefore, we characterized whether PIX decreased DOXOL levels by interfering with DOX metabolism. In isolated soluble fractions incubated with NADPH and DOX, MITOX and PIX or PIX metabolites inhibited DOXOL formation in a competitive concentration-dependent manner, i.e., inhibition was reversed upon increasing DOX concentration (not shown). With DOX at 10 µM, 50% inhibition occurred when anthracenedione:DOX ratios were approximately 30 for MITOX, 20 for PIX and CT-45886, and 2 for CT-45889 and CT-45890 (**Figure 8C**). We calculated anthracenedione:DOX ratios in the soluble fraction of strips sequentially exposed to DOX and anthracenediones. The ratios were normalized to those that caused 50% inhibition of DOXOL formation in isolated soluble fractions, and the values thereby obtained (IC_{50} percentages) were used to approximate the likelihood with which anthracenediones inhibited DOXOL formation in the strips. After DOX loading, DOX levels were too high to permit formation of significant IC_{50} percentages. After DOX loading/multiple washouts, DOX levels diminished substantially, anthracenedione:DOX ratios increased, and IC_{50} percentages could be calculated. CT-45886, the nonperoxidatic N-dealkylated metabolite of PIX, showed the highest IC_{50} percentage, followed by PIX and MITOX. CT-45889 and CT-45890 were too diffusible to generate IC_{50} percentages (**Figure 8D**). MITOX metabolites diffused completely and were assumed to have minor significance in these experiments.

In the soluble fraction of strips sequentially exposed to DOX loading/multiple washouts and PIX, DOXOL decreases correlated with CT-45886 concentrations, but not PIX concentrations (**Figure 9A**). This suggested that DOXOL formation diminished as PIX hydrolyzed to CT-45886 and the latter attained higher molar ratios to DOX. Accordingly, treating the strips with 1 µM PIX caused partial inhibition of DOXOL formation, and treating the strips with equimolar CT-45886 completely inhibited DOXOL formation (**Figure 9B**).

DISCUSSION

In comparison with MITOX, PIX exhibited higher uptake and accumulation in both DOX-naïve and DOX-loaded human myocardial strips. This cannot be explained by lipophilicity as PIX is less lipophilic than MITOX (Colombo et al., 2009). The greater accumulation of PIX may be due to its weaker binding to plasma proteins (Cell Therapeutics Inc, 2012), resulting in a higher fraction of diffusible PIX. The uptake of PIX diminished if DOX loading and PIX administration were separated by one or more washouts that stimulated DOX clearance. The greatest reduction of PIX uptake occurred when multiple washouts were used to simulate clinical situations in which patients receive DOX and eliminate it over months or years before they undergo PIX salvage therapy (Pettengell et al., 2012).

The effects of DOX clearance on reducing PIX uptake were not primarily due to facilitated interaction of PIX with MDR drug efflux pumps. Verapamil, inhibitor of P-glycoprotein and MRP1, increased accumulation of DOX but not of PIX, which was consistent with PIX being a poor substrate-inhibitor of MDR pumps as compared to DOX, MITOX, or other investigational anthracenediones (Cell Therapeutics Inc, 2012; Chou et al., 2002). It has been suggested that chemical modifications of the chromophore backbone limited PIX recognition by MDR proteins (Chou et al., 2002).

PIX uptake and accumulation were more likely diminished by membrane effects that occurred during DOX clearance. DOX moves across biologic membranes by a two-step process in which rapid passive diffusion through one side of the membrane is followed by "flip-flop" reorientation in the lipid bilayer and slow outflow from the opposite side of the membrane (Regev and Eytan, 1997). This process decreases membrane lipid order and impairs membrane penetration by other unrelated compounds (Lameh et al., 1989). PIX uptake would diminish if washouts made DOX diffuse and reorient in proximity to the membrane outer leaflet exposed to PIX. MITOX accumulation was not diminished by washouts. The higher lipophilicity of MITOX may have favoured its penetration even in a membrane environment altered by DOX clearance.

Neither PIX nor MITOX altered myocardial distribution or clearance of DOX; however, the two drugs were substantially different in terms of ROS formation. PIX did not increase the myocardial levels of DCF-detectable H_2O_2 and did not form metabolites that reflected formation and utilization of H_2O_2 in drug metabolism by cellular peroxidases. MITOX also failed to increase DCF-detectable H_2O_2, but in the presence of DOX, it formed metabolites consistent with increased production and utilization of H_2O_2 in peroxidatic drug metabolism, even in DOX loading/multiple washout experiments in which DOX levels were too low to form H_2O_2. These findings indicate that MITOX synergized with DOX to accentuate H_2O_2 formation.

Patients treated with cumulative doses of DOX may develop circulating levels of cTnI (Cardinale and Sandri, 2012). Here, myocardial strips received a single, clinically relevant dose of DOX and/or anthracenedione, which was insufficient to induce cTnI release. We reported that such conditions did not cause histologic damage of the strips (Salvatorelli, Guarnieri et al., 2006; Salvatorelli et al., 2012b). Nevertheless, a reduced cardiotoxicity of PIX versus MITOX in DOX-treated patients could be anticipated by measuring mitochondrial aconitase inactivation, a highly sensitive marker of subthreshold damage from pathophysiologic levels of $O_2^{\cdot-}$ (Gardner, 2002; Salvatorelli, Guarnieri et al., 2006; Salvatorelli et al., 2012b). PIX did not increase aconitase inactivation in the strips loaded with DOX; in contrast, MITOX exacerbated inactivation induced by DOX loading and also synergized with DOX in inducing inactivation in the strips subjected to DOX loading/multiple washouts. Peroxidatic MITOX metabolites might be electrophilic enough to substitute for $O_2^{\cdot-}$ in inactivating mitochondrial aconitase; however, this possibility should be weighed against complete elimination of such metabolites from the strips.

One-electron redox cycling of DOX and ROS formation is promoted by the NADH dehydrogenase of mitochondrial complex I, sarcoplasmic NADPH-cytochrome P450 reductase, NADPH oxidase, and other oxido-reductases (Deng et al., 2007; Doroshow, 1983; Powis, 1989; Vasquez-Vivar et al., 1997). The quinone moiety of MITOX is more electronegative than that of DOX (- 0.79 V versus -0.6 V) (Nguyen and Gutierrez, 1990). This makes MITOX a poor substrate for NAD(P)H oxidoreductases. Elimination of the electron-dense hydroquinone moiety may have

rendered the quinone moiety of PIX even more electronegative and virtually resistant to one-electron reduction. On the other hand, the data suggest that a prior exposure of the strips to DOX enabled MITOX to engage in redox reactions. DOX complexation with mitochondrial cardiolipin, and changes in the architecture and redox potential of mitochondrial electron transport system, may play a role in these settings (Salvatorelli et al., 2012b).

The lifetime risk of cardiotoxicity correlates with cardiac accumulation of DOXOL (Blanco et al., 2012; Menna et al., 2008; Minotti et al., 2010). In human myocardium, DOXOL is formed by heterogeneous families of cytoplasmic aldo-keto or carbonyl reductases (Blanco et al., 2012; Kalabus et al., 2012; Menna et al., 2008; Mordente et al., 2003; Salvatorelli, Guarnieri et al., 2006; Slupe et al., 2005). Non-anthracycline chemotherapeutics may change DOXOL formation without altering the expression level of the reductases (Salvatorelli, Menna et al., 2006). Drugs that occupy a positive regulatory site of the reductases increase DOXOL formation, while drugs that compete for the active site decrease DOXOL formation (Menna et al., 2008; Salvatorelli, Menna et al., 2006 Salvatorelli et al., 2007). PIX decreased DOXOL levels in DOX loading/multiple washout experiments that best reproduced the clinical condition of patients with a prior DOX treatment. Data from strips and isolated cytosol suggest that DOXOL formation decreased as PIX:DOX ratios increased and made PIX eventually displace DOX from the active site of reductases. Because PIX hydrolysed extensively to CT-45886 in the strips, DOXOL inhibition occurred primarily through the action of this N-dealkylated metabolite of PIX. N-cyclized metabolites, CT-45889 and CT-45890, did not form significant molar ratios with DOX and did not contribute to inhibiting DOXOL formation in the strips. Other potential metabolites of PIX were not considered; in clinical studies, minimal amounts of mono- or di- acetylated PIX were only occasionally recovered from urine of some patients (Cell Therapeutics Inc., 2012). In comparison with PIX, MITOX attained much lower levels molar ratios with DOX and showed only an insignificant trend toward inhibition of DOXOL.

Despite its higher uptake and accumulation in cardiac tissue, PIX shows many characteristics that may be salutary in the setting of prior DOX exposure: i) decreased uptake and accumulation in myocardial samples that mimicked prior DOX administration, ii) lack of effects on the levels and distribution of residual DOX, iii) failure to generate ROS, iv) inhibition

of DOXOL formation. This information should be tempered by unavoidable study limitations. Months to years after the last anthracycline administration, progressive DOX clearance or conversion to DOXOL should generate roughly identical myocardial levels of DOX and DOXOL (Stewart et al., 1993); in contrast, strips subjected to DOX loading/multiple washouts still contained much more DOX than DOXOL. In addition, our model reproduces pharmacologic events associated with just one PIX administration, while the cardiac toxicity of a drug is usually cumulative, increasing with additional doses or regimens. Multiple doses of DOX cause a mitochondriopathy that results in ROS formation even after completion of chemotherapy (Minotti et al., 2012; Lebrecht and Walker, 2007); this cannot be characterized by our model. Nonetheless, our data show that PIX was redox inactive and inhibited DOXOL formation in the face of significant levels of residual DOX. MITOX did not inhibit DOXOL formation, but synergized with DOX to form more ROS.

These data provide a biological rationale for the cardiac safety of PIX in patients with prior DOX therapy. Moreover, it is known that in cancer cells the mode of action of PIX was not confined to inhibiting topoisomerase II but extended to forming PIX-formaldehyde conjugates that cross-linked to DNA much more efficaciously than equivalent DOX conjugates (Cell Therapeutics Inc., 2012; Evison et al., 2009). This anticipates that in cancer cells altered by prior waves of DOX clearance, a limited uptake of PIX would be outweighed by its greater potency in damaging DNA.

Lack of intramyocardial toxic bioactivation suggests that PIX could be of value also as first-line agent. In a phase II study that compared CHOP-rituximab with CP(ixantrone)OP-rituximab in chemotherapy-naïve patients with DLBCL, CPOP-rituximab caused similar rates of progression free survival but induced lower rates of serious cardiac events (Herbrecht et al., 2011). Interestingly). Patients treated with CPOP-rituximab were also shown to develop fewer troponin elevations over the course of therapy (Cell Therapeutics Inc., data on file). This denoted that in patients exposed to cumulative doses of drugs, PIX was safer than DOX and spared the heart from the summation of toxic insults. It will be important to establish whether PIX also caused fewer elevations of natriuretic peptides that signal hemodynamic stress, cardiomyocyte stretch, and

ventricle dilation or hypertrophy (Braunwald, 2008). This could not be established in our short-term studies of isolated myocardial samples.

In conclusion, PIX differs from both DOX and MITOX in a translational model of human myocardium. This information endorses development of PIX as a new agent for active and safe therapy for NHL.

AUTHORSHIP CONTRIBUTIONS

Participated in research design: E. Salvatorelli, P. Menna, G. Minotti

Conducted experiments: E. Salvatorelli, P. Menna, O. Gonzalez Paz

Contributed new reagents or analytic tools: E. Salvatorelli, P. Menna, M. Chello, E. Covino

Performed data analysis: E. Salvatorelli, P. Menna, G. Minotti

Wrote or contributed to the writing of the manuscript: E. Salvatorelli, P. Menna, J.W. Singer, G.

Minotti

REFERENCES

Barry E, Alvarez JA, Scully RE, Miller TL and Lipshultz SE (2007) Anthracycline-induced cardiotoxicity: course, pathophysiology, prevention and management. *Expert Opin Pharmacother* **8**: 1039-1058.

Blanco JG, Sun CL, Landier W, Chen L, Esparza-Duran D, Leisenring W, Mays A, Friedman DL, Ginsberg JP, Hudson MM, Neglia JP, Oeffinger KC, Ritchey AK, Villaluna D, Relling MV and Bhatia S (2012) Anthracycline-related cardiomyopathy after childhood cancer: role of polymorphisms in carbonyl reductase genes-a report from the Children's Oncology Group. *J Clin Oncol* **30**: 1415-1421.

Blanz J, Mewes K, Ehninger G, Proksch B, Waidelich D, Greger B and Zeller KP (1991) Evidence for oxidative activation of mitoxantrone in human, pig, and rat. *Drug Metab Dispos* **19**: 871-880.

Borchmann P, Schnell R, Knippertz R, Staak JO, Camboni GM, Bernareggi A, Hübel K, Staib P, Schulz A, Diehl V and Engert A (2001) Phase I study of BBR 2778, a new aza-anthracenedione, in advanced or refractory non-Hodgkin's lymphoma. *Ann Oncol* **12**: 661-667.

Budde T, Haney J, Bien S, Schwebe M, Riad A, Tschöpe C, Staudt A, Jedlitschky G, Felix SB, Kroemer HK, and Grube M (2011) Acute exposure to doxorubicin results in increased cardiac P-glycoprotein expression. *J Pharm Sci* **100**: 3951-3958.

Braunwald E (2008) Biomarkers in heart failure. *N Engl J Med* **358**: 2148-2159.

Canal P, Attal M, Chatelut E, Guichard S, Huguet F, Muller C, Schlaifer D, Laurent G, Houin G and Bugat R (1993) Plasma and cellular pharmacokinetics of mitoxantrone in high-dose chemotherapeutic regimen for refractory lymphomas. *Cancer Res* **53**: 4850-4854.

Cardinale D and Sandri MT (2012) Role of biomarkers in chemotherapy-induced cardiotoxicity. *Prog Cardiovasc Dis* **53**: 121-129.

Cavalletti E, Crippa L, Mainardi P, Oggioni N, Cavagnoli R, Bellini O and Sala F (2007) Pixantrone (BBR 2778) has reduced cardiotoxic potential in mice pretreated with doxorubicin: comparative studies against doxorubicin and mitoxantrone. *Invest New Drugs* **25**: 87-95.

Cell Therapeutics Inc (2010) Pixantrone (BBR 2778) versus other chemotherapeutic agents for third-line single agent treatment of patients with relapsed aggressive non-Hodgkin's lymphoma: A randomized, controlled, phase III comparative trial. CTI Study Report PIX301 PK.

Cell Therapeutics Inc (2012) Pixantrone dimaleate (BBR 2778). Investigator Brochure Version 12.

Chance B, Sies H, and Boveris A (1979) Hydroperoxide metabolism in mammalian organs. *Physiol Rev* **59**: 527-605.

Chou KM, Krapcho AP, Horn D and Hacker M (2002) Characterization of anthracenediones and their photoaffinity analogs. *Biochem Pharmacol* **63**: 1143-1147.

Colombo R, Carotti A, Catto M, Racchi M, Lanni C, Verga L, Caccialanza G and De Lorenzi E (2009) CE can identify small molecules that selectively target soluble oligomers of amyloid beta protein and display antifibrillogenic activity. *Electrophoresis* **30**: 1418-1429.

Deng S, Kruger A, Kleschyov AL, Kalinowski L, Daiber A and Wojnowski L (2007) Gp91phox-containing NADPH oxidase increases superoxide formation by doxorubicin and NADPH. *Free Radic Biol Med* **42**: 466-473.

Doroshow JH (1983) Anthracycline antibiotic-stimulated superoxide hydrogen peroxide and hydroxyl radical production by NADH dehydrogenase. *Cancer Res* **43**: 4543–4551.

Evison BJ, Bilardi RA, Chiu FC, Pezzoni G, Phillips DR, and Cutts SM (2009) CpG methylation potentiates pixantrone and doxorubicin-induced DNA damage and is a marker of drug sensitivity. *Nucleic Acids Res* **37**: 6355-6370.

Faulds D, Balfour JA, Chrisp P and Langtry HD (1991) Mitoxantrone. A review of its pharmacodynamic and pharmacokinetic properties, and therapeutic potential in the chemotherapy of cancer. *Drugs* **4**: 400-449.

Flens MJ, Zaman GJ, van der Valk P, Izquierdo MA, Schroeijers AB, Scheffer GL, van der Groep P, de Haas M, Meijer CJ, and Scheper RJ (1996) Tissue distribution of the multidrug resistance protein. *Am J Pathol* **148**: 1237-1247.

Gardner PR (2002) Aconitase: sensitive target and measure of superoxide. *Methods Enzymol* **349**: 9-23.

Gewirtz DA (1999) A critical evaluation of the mechanisms of action proposed for the antitumor effects of the anthracycline antibiotics adriamycin and daunorubicin. *Biochem Pharmacol* **57**: 727-741.

Gianni L, Viganò L, Locatelli A, Capri G, Giani A, Tarenzi E and Bonadonna G (1997) Human pharmacokinetic characterization and in vitro study of the interaction between doxorubicin and paclitaxel in patients with breast cancer. *J Clin Oncol* **15**: 1906-1915.

Herbrecht R, MacDonald D, Weissinger F, Wilhelm M, Holladay C, Dang NH, Holman P, Cernohous P, Singer J and van der Jagt RH (2011) CPOP-R versus CHOP-R as first-line therapy for diffuse large B-cell lymphoma (DLBCL): A phase 2, randomized, open-label, multicenter study. *Blood* **118**: 1605A.

Kalabus JL, Sanborn CC, Jamil RG, Cheng Q and Blanco JG (2012) Expression of the anthracycline-metabolizing enzyme carbonyl reductase 1 in hearts from donors with Down syndrome. *Drug Metab Dispos* **38**: 2096-2099.

Kalyanaraman B, Darley-Usmar V, Davies KJ, Dennery PA, Forman HJ, Grisham MB, Mann GE, Moore K, Roberts LJ 2nd, and Ischiropoulos H (2012) Measuring reactive oxygen and nitrogen species with fluorescent probes: challenges and limitations. *Free Radic Biol Med* **52**:1-6.

Lameh J, Chuang RY, Israel M and Chuang LF (1989) Nucleoside uptake and membrane fluidity studies on N-trifluoroacetyladriamycin-14-O-hemiadipate-treated human leukemia and lymphoma cells. *Cancer Res* **49**: 2905-2908.

LeBel CP, Ischiropoulos H and Bondy SC (1992) Evaluation of the probe 2',7'-dichlorofluorescin as an indicator of reactive oxygen species formation and oxidative stress. *Chem Res Toxicol* **5**: 227-231.

Lebrecht D and Walker UA (2007) Role of mtDNA lesions in anthracycline cardiotoxicity. *Cardiovasc Toxicol* **7**: 108-113.

Meissner K, Jedlitschky G, Meyer zu Schwabedissen H, Dazert P, Eckel L, Vogelgesang S, Warzok RW, Böhm M, Lehmann C, Wendt M, Cascorbi I, Kroemer HK (2004) Modulation of

multidrug resistance P-glycoprotein 1 (ABCB1) expression in human heart by hereditary polymorphisms. *Pharmacogenetics* **14**: 381-385.

Menna P, Salvatorelli E and Minotti G (2008) Cardiotoxicity of antitumor drugs. *Chem Res Toxicol* **15**: 1179-1189.

Minotti G, Menna P, Salvatorelli E, Cairo G and Gianni L (2004) Anthracyclines: Molecular advances and pharmacologic developments in antitumor activity and cardiotoxicity. *Pharmacol Rev* **56**: 185-229.

Minotti G, Recalcati S, Menna P, Salvatorelli E, Corna G and Cairo G (2004) Doxorubicin cardiotoxicity and the control of iron metabolism: quinone-dependent and independent mechanisms. *Methods Enzymol* **378**: 340-361.

Minotti G, Salvatorelli E and Menna P (2012) Pharmacological foundations of cardio-oncology. *J Pharmacol Exp Ther* **334**: 2-8.

Mordente A, Minotti G, Martorana GE, Silvestrini A, Giardina B and Meucci E (2003) Anthracycline secondary alcohol metabolite formation in human or rabbit heart: Biochemical aspects and pharmacologic implications. *Biochem Pharmacol* **66**: 989-998.

Motzer RJ, Lyn P, Fischer P, Lianes P, Ngo RL, Cordon-Cardo C, and O'Brien JP (1995) Phase I/II trial of dexverapamil plus vinblastine for patients with advanced renal cell carcinoma. *J Clin Oncol* **13**: 1958-1965.

Mushlin PS, Cusack BJ, Boucek RJ Jr, Andrejuk T, Li X and Olson RD (1993) Time-related increases in cardiac concentrations of doxorubicinol could interact with doxorubicin to depress myocardial contractile function. *Br J Pharmacol* **110**: 975-982.

Nguyen B and Gutierrez PL (1990) Mechanism(s) for the metabolism of mitoxantrone: electron spin resonance and electrochemical studies. *Chem Biol Interact* **74**: 39-62.

Osby E, Hagberg H, Kvaløy S, Teerenhovi L, Anderson H, Cavallin-Stahl E, Holte H, Myhre J, Pertovaara H and Björkholm M (2003) CHOP is superior to CNOP in elderly patients with aggressive lymphoma while outcome is unaffected by filgrastim treatment: results of a Nordic Lymphoma Group randomized trial. *Blood* **101**: 3840-3848.

Pettengell R, Coiffier B, Narayanan G, de Mendoza FH, Digumarti R, Gomez H, Zinzani PL, Schiller G, Rizzieri D, Boland G, Cernohous P, Wang L, Kuepfer C, Gorbatchevsky I and Singer JW (2012) Pixantrone dimaleate versus other chemotherapeutic agents as a single-agent salvage treatment in patients with relapsed or refractory aggressive non-Hodgkin lymphoma: a phase 3, multicentre, open-label, randomised trial. *Lancet Oncol* **13**: 696-706.

Powis G (1989) Free radical formation by antitumor quinones. *Free Radic Biol Med* **6**: 63-101.

Regev R and Eytan GD (1997) Flip-flop of doxorubicin across erythrocyte and lipid membranes. *Biochem Pharmacol* **54**: 1151-1158.

Reszka KJ, Matuszak Z and Chignell CF (1997) Lactoperoxidase-catalyzed oxidation of the anticancer agent mitoxantrone by nitrogen dioxide (NO_2) radicals. *Chem Res Toxicol* **10**: 1325-1330.

Reszka KJ, Sallans L, Macha S, Brown K, McGraw DW, Kovacic MB and Britigan BE (2011) Airway peroxidases catalyze nitration of the β_2-agonist salbutamol and decrease its pharmacological activity. *J Pharmacol Exp Ther* **336**: 440-449.

Rota C, Fann YC, and Mason RP (1999) Phenoxyl free radical formation during the oxidation of the fluorescent dye 2',7'-dichlorofluorescein by horseradish peroxidase. Possible consequences for oxidative stress measurements. *J Biol Chem* **274**: 28161-28168.

Salvatorelli E, Guarnieri S, Menna P, Liberi G, Calafiore AM, Mariggiò MA, Mordente A, Gianni L and Minotti G (2006) Defective one or two electron reduction of the anticancer anthracycline epirubicin in human heart: Relative importance of vesicular sequestration and impaired efficiency of electron addition. *J Biol Chem* **281**: 10990-11001.

Salvatorelli E, Menna P, Cascegna S, Liberi G, Calafiore AM, Gianni L and Minotti G (2006) Paclitaxel and docetaxel stimulation of doxorubicinol formation in the human heart: implications for cardiotoxicity of doxorubicin-taxane chemotherapies. *J Pharmacol Exp Ther* **318**: 424-433.

Salvatorelli E, Menna P, Gianni L and Minotti G (2007) Defective taxane stimulation of epirubicinol formation in the human heart: Insight into the cardiac tolerability of epirubicin-taxane chemotherapies. *J Pharmacol Exptl Ther* **320**: 790-800.

Salvatorelli E, Menna P, Lusini M, Covino E and Minotti G (2009) Doxorubicinolone formation and efflux: a salvage pathway against epirubicin accumulation in human heart. *J Pharmacol Exp Ther* **329**: 175-184.

Salvatorelli E, Menna P, Surapaneni S, Aukerman SL, Chello M, Covino E, Sung V and Minotti G (2012a) Pharmacokinetic characterization of amrubicin cardiac safety in an ex vivo human myocardial strip model. I. Amrubicin accumulates to a lower level than doxorubicin or epirubicin. *J Pharmacol Exp Ther* **341**: 464-473.

Salvatorelli E, Menna P, Gonzalez Paz O, Surapaneni S, Aukerman SL, Chello M, Covino E, Sung V and Minotti G (2012b) Pharmacokinetic characterization of amrubicin cardiac safety in an ex vivo human myocardial strip model. II. Amrubicin shows metabolic advantages over doxorubicin and epirubicin. *J Pharmacol Exp Ther* **341**: 474-483.

Slupe A, Williams B, Larson C, Lee LM, Primbs T, Bruesch AJ, Bjorklund C, Warner DL, Peloquin J, Shadle SE, Gambliel HA, Cusack BJ, Olson RD and Charlier HA Jr (2005) Reduction of 13-deoxydoxorubicin and daunorubicinol anthraquinones by human carbonyl reductase. *Cardiovasc Toxicol* **5**: 365-376.

Sonneveld P, de Ridder M, van der Lelie H, Nieuwenhuis K, Schouten H, Mulder A, van Reijswoud I, Hop W and Lowenberg B (1995) Comparison of doxorubicin and mitoxantrone in the treatment of elderly patients with advanced diffuse non-Hodgkin's lymphoma using CHOP versus CNOP chemotherapy. *J Clin Oncol* **13**: 2530-2539.

Stewart DJ, Grewaal D, Green RM, Mikhael N, Goel R, Montpetit VA and Redmond MD (1993) Concentrations of doxorubicin and its metabolites in human autopsy heart and other tissues. *Anticancer Res* **13**: 1945-1952.

Stoscheck CM (1990) Quantitation of protein. *Methods Enzymol* **182**: 50-68.

Swain SM, Whaley FS and Ewer MS (2003) Congestive heart failure in patients treated with doxorubicin: a retrospective analysis of three trials. *Cancer* **97**: 2869-2879.

Vasquez-Vivar J, Martasek P, Hogg N, Masters BS, Pritchard KA Jr and Kalyanaraman B (1997) Endothelial nitric oxide synthase-dependent superoxide generation from adriamycin. *Biochemistry* **36**: 11293-11297.

Vellonen K-S, Honkakoski P and Urtti A (2004) Substrates and inhibitors of efflux proteins interfere with the MTT assay in cells and may lead to underestimation of drug toxicity. *Eur J Pharm Sci* **23**: 181-188.

Warner E, Hedley D, Andrulis I, Myers R, Trudeau M, Warr D, Pritchard KI, Blackstein M, Goss PE, Franssen E, Roche K, Knight S, Webster S, Fraser RA, Oldfield S, Hill W, and Kates R (1998) Phase II study of dexverapamil plus anthracycline in patients with metastatic breast cancer who have progressed on the same anthracycline regimen. *Clin Cancer Res* **4**: 1451-1457.

Whitaker G, Lillquist A, Pasas SA, O'Connor R, Regan F, Lunte CE and Smyth MR (2008) CE-LIF method for the separation of anthracyclines: application to protein binding analysis in plasma using ultrafiltration. *J Sep Sci* **31**: 1828-1833.

FOOTNOTES

32

FIGURE LEGENDS

Figure 1 <u>Structures of DOX, PIX, and MITOX</u>

DOX is composed of a tetracyclic quinone-hydroquinone chromophore and a carbonyl-containing side chain, liable to two-electron reduction to DOXOL (indicated by arrow). MITOX is a three ring quinone-hydroquinone anthracenedione; its side chains lack carbonyl groups. PIX differs from MITOX in the lack of the hydroquinone, insertion of a nitrogen heteroatom in the same ring, and substitution of (ethylamino)-diethylamino for (hydroxyethylamino)-ethylamino side chains (all indicated by arrows).

Figure 2 <u>Anthracenedione levels in DOX-loaded myocardial strips</u>

Panel A: flowchart for probing anthracenediones as single-agents (a) or in sequence with DOX loading (b), DOX loading and washout (c), DOX loading and multiple washouts (d). Panels B-D: anthracenedione levels in human myocardial strips exposed to PIX or MITOX alone or in sequence with DOX (same captions as in panel A). The values are means ± SE of 9-16 experiments.

Panel B shows total anthracenedione levels (membrane fraction + soluble fractions); panel C and D show, respectively, anthracenedione levels in membrane or soluble fractions.

[*]P<0.01 versus single-agent MITOX (unpaired Student's t test), [**]P<0.05 versus PIX alone or PIX after DOX loading, [***]P<0.05 versus PIX after DOX loading/washout (one-way ANOVA followed by Bonferroni's test for multiple comparisons), [†]P<0.05 versus MITOX after DOX loading/multiple washouts (unpaired Student's t test).

Figure 3 PIX uptake, clearance, and accumulation, in human myocardial strips sequentially loaded with DOX and PIX under conditions of continuous DOX efflux

In panels A-C, human myocardial strips were loaded for 30 min with 1 or 10 µM DOX. Following one washout, PIX was added for 30 min at 1 µM; following one more washout, the incubations were allowed to proceed for a total length of 2.5 h. Strips exposed to only PIX served as controls. At the end of the experiments, the strips were assayed for PIX uptake (accumulation + cumulative efflux), clearance (cumulative efflux:uptake), and accumulation. Values were means ± SE (n=9); [*]denotes significantly lower compared to strips exposed to PIX only (one-way ANOVA followed by Bonferroni's test for multiple comparisons).

In panel D, the strips were subjected to DOX loading with 10 µM DOX, followed by multiple washouts and PIX addition. Where indicated, 1 µM verapamil was included after the last washout and allowed to equilibrate for 5 min before PIX was added. Values were means of 3-7 experiments in triplicate; [**]denotes significantly lower compared to strips without verapamil ($P < 0.05$ by unpaired Student's t test).

Figure 4 PIX metabolism in myocardial strips

Strips were incubated with PIX as single agent or in sequence with DOX loading or DOX loading/multiple washouts (captions as in Figure 2). Grey circles indicate PIX dealkylation or side chain cyclization. The values (means ± SE, n=3-6) were expressed as total metabolite (metabolite in strips + metabolite in plasma). [*]$P<0.05$ versus CT-45889 or CT-45890 (one-way ANOVA followed by Bonferroni's test for multiple comparisons); [†]$P<0.025$ versus PIX single-agent or in sequence with DOX loading (unpaired Student's t test).

Figure 5 MITOX metabolism in myocardial strips

Strips were incubated with MITOX as single agent or in sequence with DOX loading or DOX loading/multiple washouts. Grey circles show hydroquinone oxidation and/or side chain N-cyclization and/or C-terminus carboxylation or peroxidation. Metabolites were ranked according to

their degree of oxidation. Metabolites D and E exhibited the same molecular mass and therefore, could not be distinguished. The figure is representative of three experiments.

Figure 6 Apparent versus theoretical PIX accumulation in human myocardial strips

PIX or MITOX was used as single agent or in sequence with DOX. Captions were as in Figure 2: a, single-agent PIX or MITOX; b, PIX or MITOX added in sequence with DOX loading and washout; d, PIX or MITOX added in sequence with DOX loading and multiple washouts. MITOX accumulation was not influenced by metabolite retention; instead, PIX accumulation was influenced by formation and incomplete diffusion of CT-45886. Apparent accumulation denoted accumulation determined by measuring PIX only, while theoretical accumulation denoted accumulation calculated by the sum of PIX accumulation with CT-45886 accumulation. [*]$P<0.05$ for theoretical PIX accumulation vs apparent PIX accumulation in the corresponding strips; [†]$P<0.05$ for (d) vs (a) or (b) (unpaired Student's t test).

Figure 7 Myocardial cTnI release or mitochondrial aconitase inactivation

Panels A-B, cTnI release; panels C-D, mitochondrial aconitase inactivation.

Experimental conditions were: 1, no drug; 2, anthracenedione; 3, DOX loading; 4, DOX loading followed by anthracenedione; 5, DOX loading and multiple washouts; 6, DOX loading and multiple washouts followed by anthracenedione. Where indicated, the strips were incubated with only 100 μM H_2O_2. Values were means ± SE of three experiments.

Panel C: [*]$P<0.05$ versus samples 1, 2, and 5 (one-way ANOVA followed by Bonferroni's test for multiple comparisons); [†]$P<0.01$ versus samples 3 and 6 (unpaired Student's t test).

Panel D: [*]$P<0.05$ versus all other samples (one-way ANOVA followed by Bonferroni's test for multiple comparisons).

Figure 8 Effects of anthracenediones on DOXOL formation in human myocardial strips

Panel A: DOX and DOXOL levels in the soluble fraction of strips exposed to DOX loading, DOX loading and washout, DOX loading and multiple washouts.

Panel B: After DOX loading and multiple washouts, DOXOL formation was significantly inhibited by the addition of PIX but not of MITOX. Values were means ± SE of 7-12 experiments. [*]$P<0.05$ versus all other samples (one-way ANOVA followed by Bonferroni's test for multiple comparisons); [†]$P<0.05$ for PIX versus MITOX (unpaired Student's t test).

Panel C: Isolated soluble fractions (0.6 mg prot./ml) were incubated with NADPH (0.25 mM) and DOX (10 μM) in Tris-HCl, pH 7.0, in the absence or presence of increasing concentrations of anthracenediones. After 4 h at 37 °C, DOXOL control values were 0.12 ± 0.02 nmol/mg prot. (n=7 experiments in triplicate); the figure shows anthracenedione:DOX ratios that caused 50% inhibition of DOXOL formation (n=3). [*]$P<0.05$ versus MITOX (unpaired Student's t test); [**]$P<0.05$ versus MITOX, PIX, CT-45886 (one-way ANOVA followed by Bonferroni's test for multiple comparisons).

Panel D: IC_{50} percentages attained by anthracenediones in the soluble fractions of strips after DOX loading or DOX loading/multiple washouts. Values were means ± SE of 3-4 experiments in triplicate. [*]$P<0.05$ versus MITOX (unpaired Student's t test); [**]$P<0.05$ versus MITOX and PIX (one-way ANOVA followed by Bonferroni's test for multiple comparisons).

Figure 9 Effects of PIX or CT-45886 on DOXOL formation in human myocardial strips

Panel A: DOXOL levels versus PIX or CT-45886 levels in the soluble fraction of strips sequentially exposed to DOX loading/multiple washouts and PIX.

Panel B: DOXOL levels in strips sequentially exposed to DOX loading/multiple washouts and PIX or CT-45886 at 1 μM (n=3). [*]$P<0.05$ versus control (one-way ANOVA followed by Bonferroni's test for multiple comparisons).

Table 1

Doxorubicin uptake, clearance, and accumulation, in human myocardial strips sequentially exposed to DOX and PIX or MITOX.

Experimental condition	DOX uptake (µM)	DOX clearance (%)	DOX accumulation		
			membrane fraction	soluble fraction (µM)	total
DOX loading	n.a.	n.a.	19.8 ± 2.2	10.0 ± 0.5	29.8 ± 2.4
+ MITOX	n.a.	n.a	16.3 ± 1.3	8.8 ± 0.6	25.1 ± 1.6
+ PIX	n.a	n.a.	18.4 ± 1.4	9.8 ± 0.4	28.2 ± 1.7
DOX loading and washout	17.1 ± 1.3	37.4 ± 1.4	7.7 ± 0.6	3.2 ± 0.4	10.9 ± 1.0*
+ MITOX	15.5 ± 0.9	39.6 ± 1.8	6.9 ± 0.5	2.5 ± 0.2	9.4 ± 0.7
+ PIX	15.8 ± 1.2	39.1 ± 1.5	7.3 ± 0.7	2.5 ± 0.3	9.6 ± 1.2
DOX loading and multiple washouts	16.1 ± 1.0	59.1 ± 1.2†	4.9 ± 0.4	1.8 ± 0.2	6.7 ± 0.6**
+ MITOX	15.4 ± 0.8	59.5 ± 1.1	4.6 ± 0.2	1.5 ± 0.1	6.1 ± 0.2
+ PIX	18.7 ± 1.6	58.8 ± 0.6	5.7 ± 0.5	2.0 ± 0.2	7.7 ± 0.7

Human myocardial strips were loaded with DOX as described in Materials and Methods and Figure 2A. After 2.5 h, MITOX or PIX was added. DOX uptake, clearance, and accumulation, were determined as described in Materials and Methods. The values were means ± SE of 9-16 experiments.

*$P<0.05$ vs DOX loading, and **$P<0.05$ vs DOX loading or DOX loading and washout (one way ANOVA followed by Bonferroni's test for multiple comparisons).
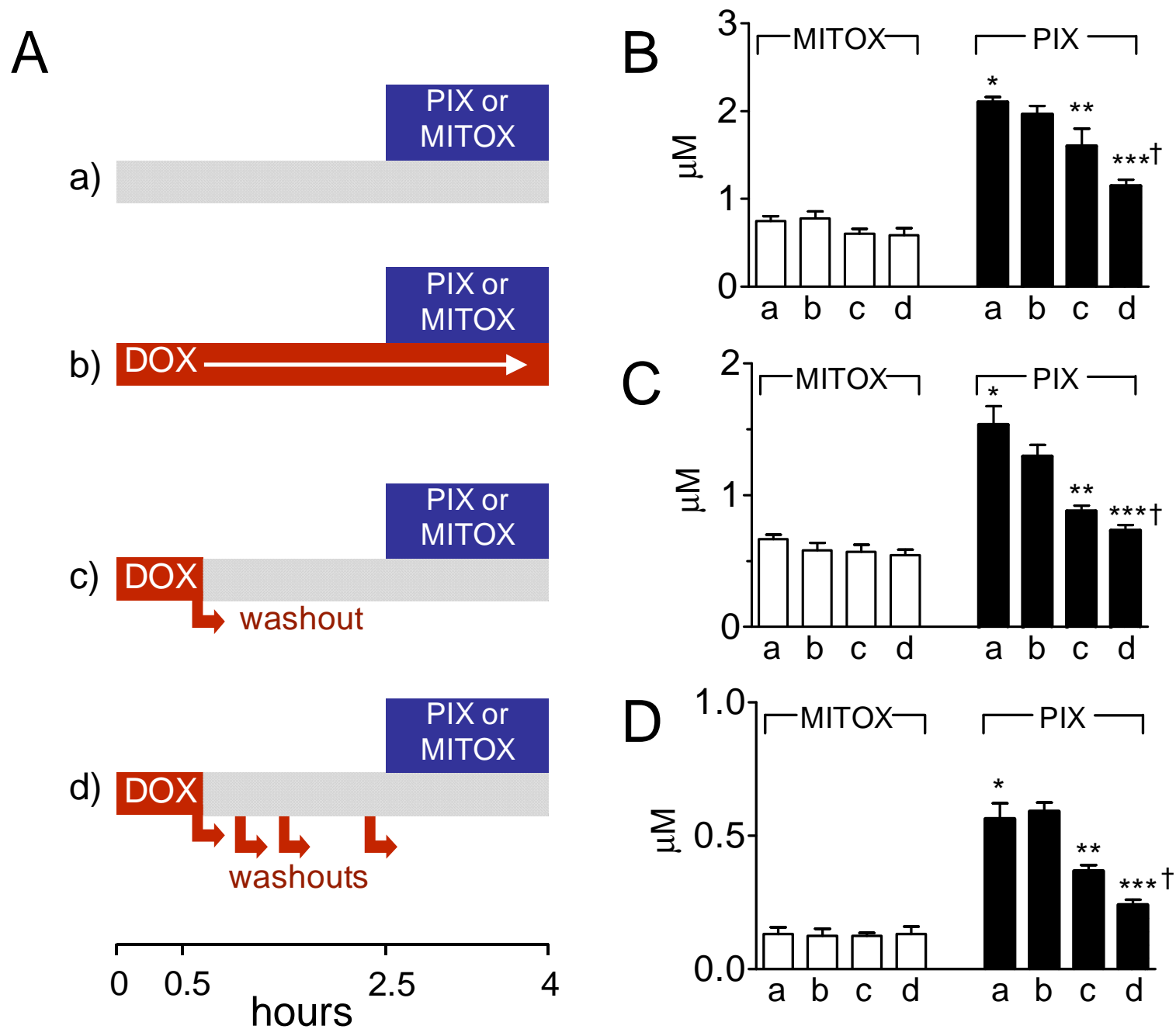
$^\dagger P<0.01$ vs loading and washout (unpaired Student's t test).

n.a., not assessable under conditions of DOX loading.

37

Table 2

Single agent anthracenedione uptake, clearance, and accumulation, in human myocardial strips

Experimental condition	Anthracenedione	Uptake (µM)	Clearance (%)	accumulation (µM)
loading	MITOX	n.a.	n.a	0.75 ± 0.05
	PIX	n.a.	n.a	2.10 ± 0.06*
loading and multiple washouts	MITOX	1.1 ± 0.04	53 ± 3.3	0.53 ± 0.05
	PIX	2.7 ± 0.04†	69 ± 0.1†	0.84 ± 0.03†

Human myocardial strips were incubated with plasma for 2.5 h; next, PIX or MITOX was added at 1 µM. In the loading condition, the incubations were allowed to proceed for 1.5 more hours without further interventions (total incubation length, 4 h). In the loading and multiple washout condition, plasma was replaced fresh at 3 and 3.5 h, and the incubation were allowed to proceed without further interventions for 30 more min (total incubation length, 4h). At the end of the experiments, the strips were assayed for PIX uptake (accumulation + cumulative efflux), clearance (cumulative efflux:uptake), and accumulation. Values were means ± SE of triplicate experiments.

(*)Denotes PIX accumulation significantly higher than MITOX accumulation under loading conditions ($P < 0.001$);

($\dagger$)denotes PIX uptake, or clearance, or accumulation, significantly higher compared to MITOX ($P < 0.001$).

n.a., not assessable under conditions of standard loading.

Table 3

Effects of PIX or MITOX on H_2O_2 levels in human myocardial strips

Anthracenedione	H_2O_2[a]		
	control	DOX loading	DOX loading + multiple washouts
	(μM)		
none	0.21 ± 0.01	0.35 ± 0.03*	0.20 ± 0.02
MITOX	0.23 ± 0.01	0.36 ± 0.02*	0.20 ± 0.02
PIX	0.22 ± 0.02	0.32 ± 0.03*	0.22 ± 0.01

[a]membrane fraction + soluble fraction.

Human myocardial strips were loaded with DCFH-DA and incubated with plasma only or subjected to DOX loading, or DOX loading followed by multiple washouts. After 2.5 h, MITOX or PIX was added at 1 μM. The values were means ± SE of 4-12 experiments.

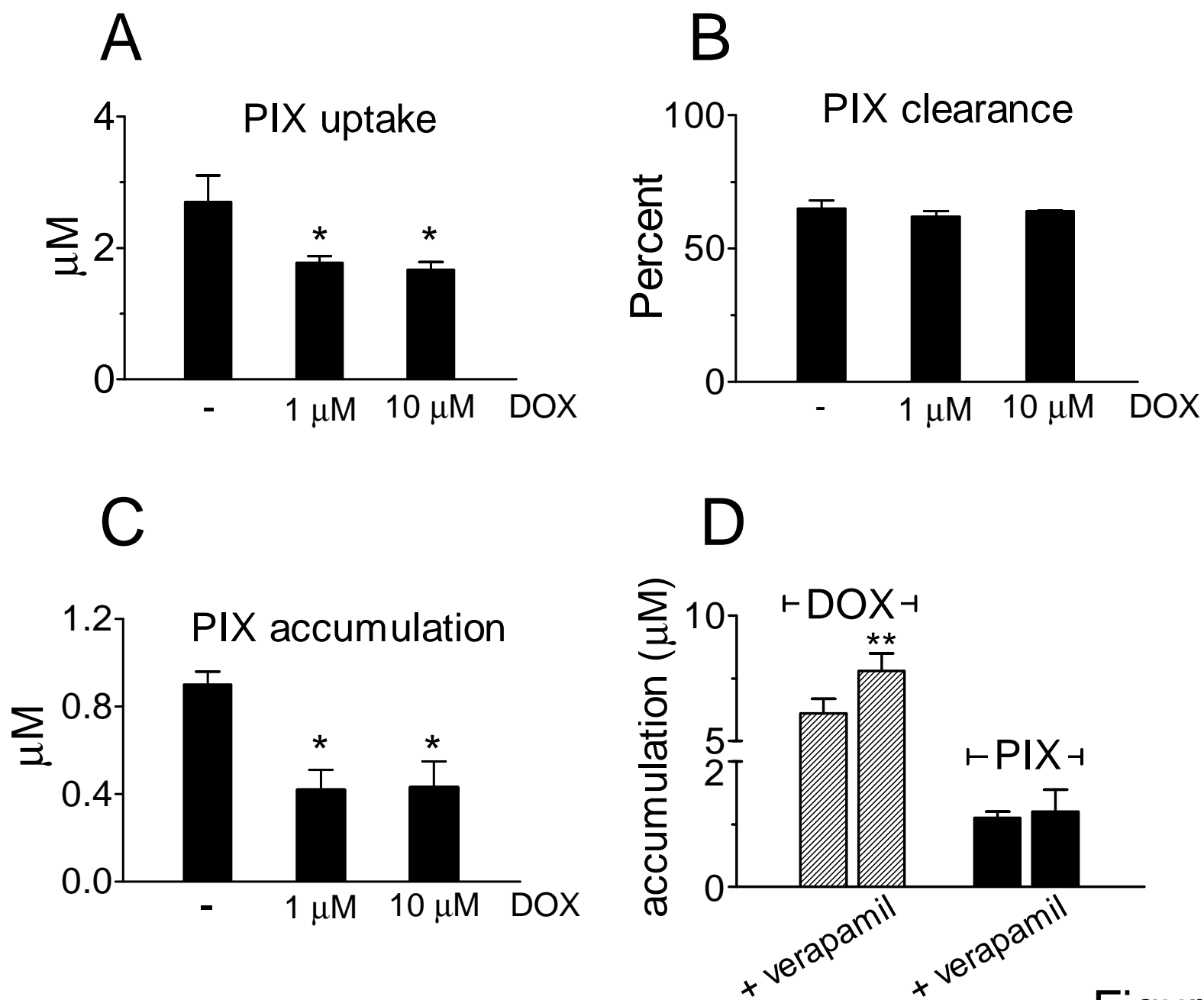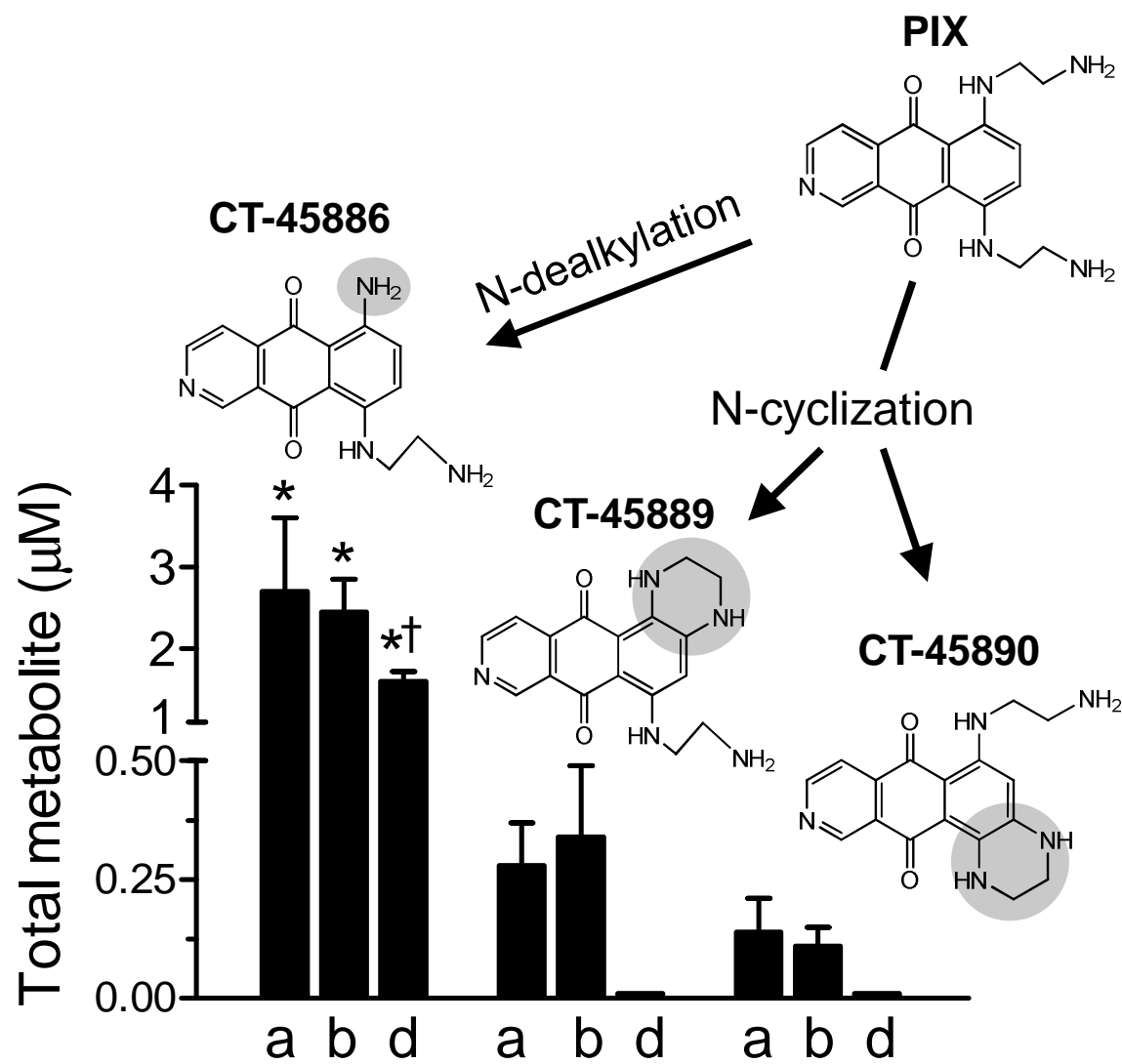*$P < 0.05$ vs control or DOX loading/multiple washouts (one-way ANOVA followed by Bonferroni's test for multiple comparisons).
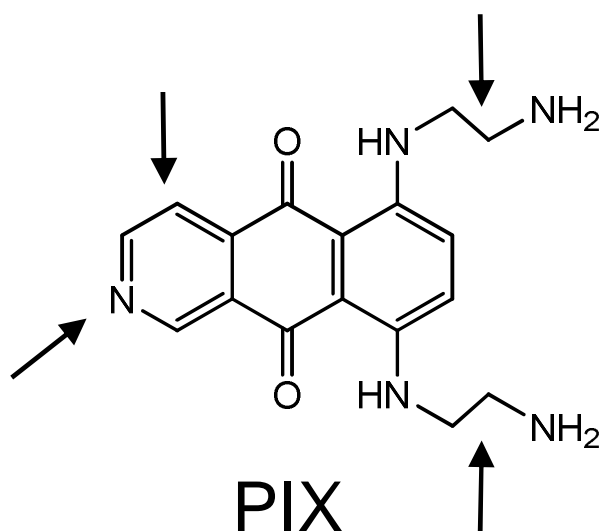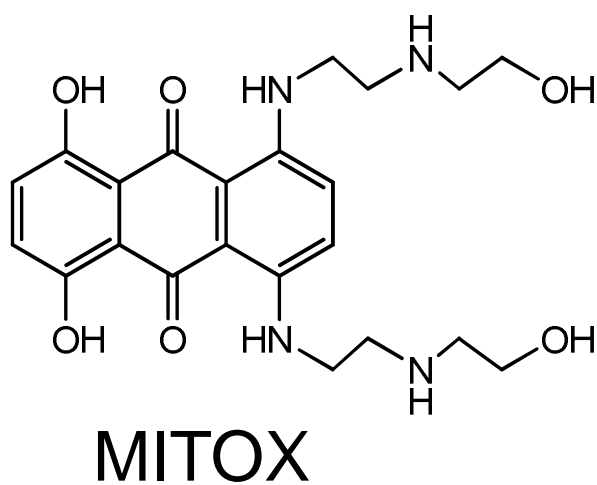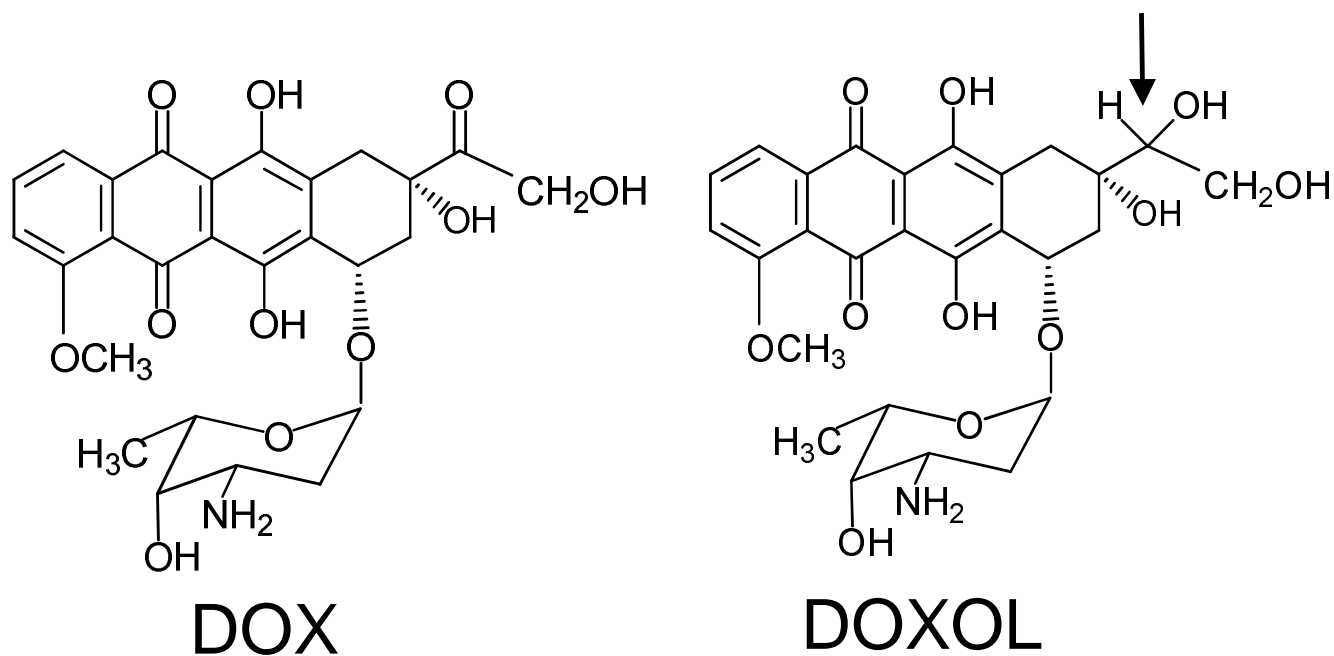
Figure 1

Figure 2

Figure 3

Figure 4

MITOX

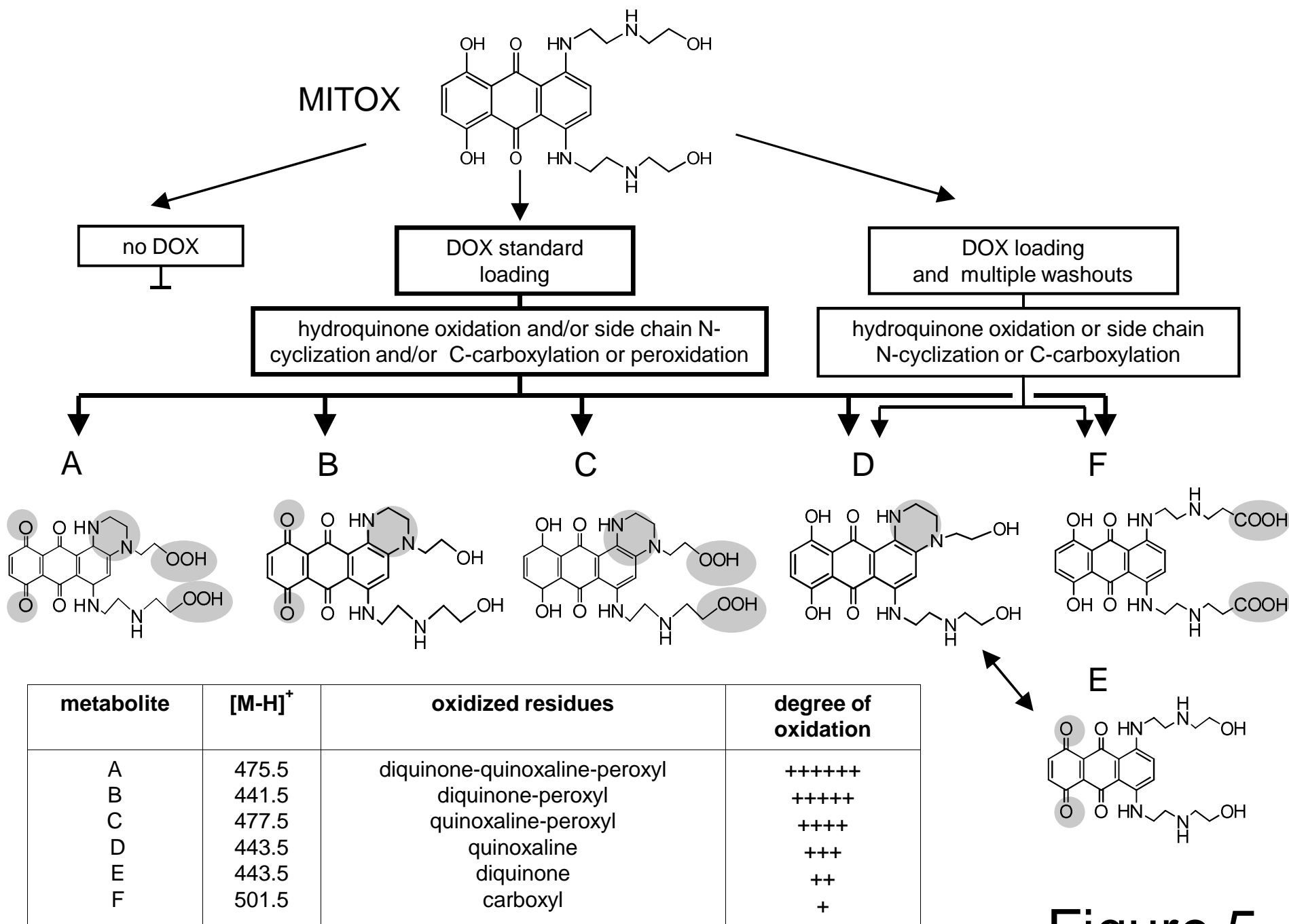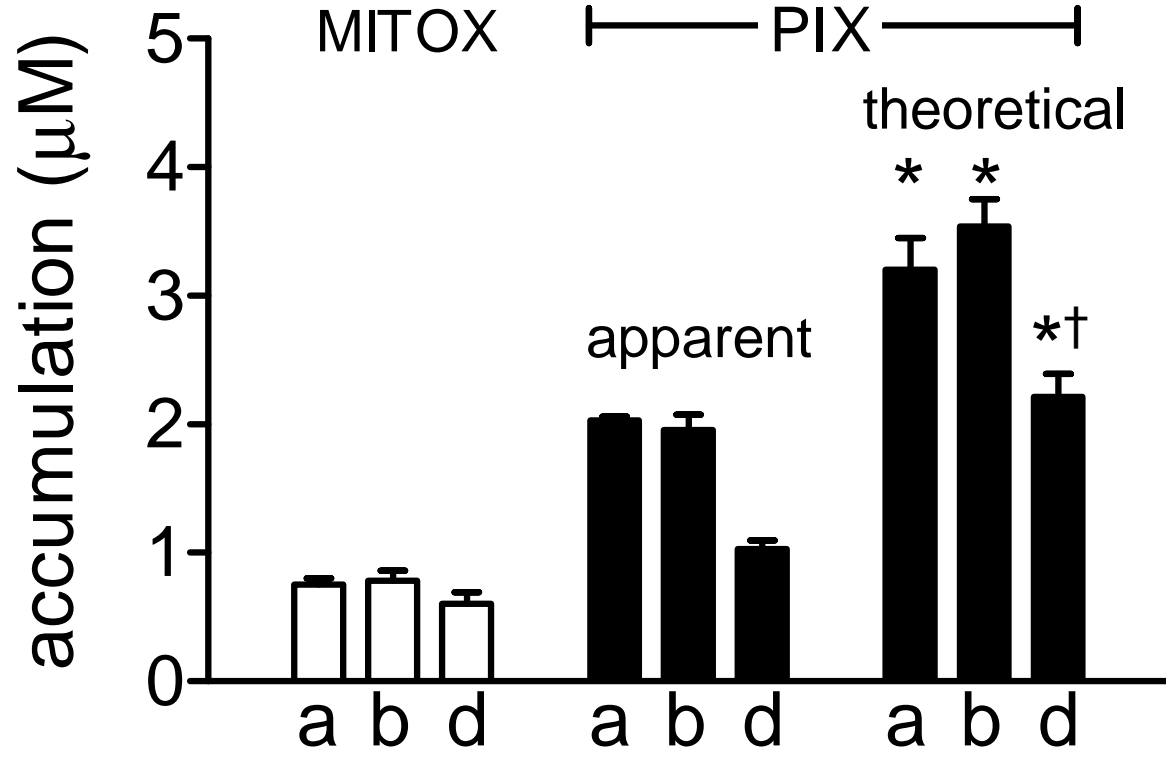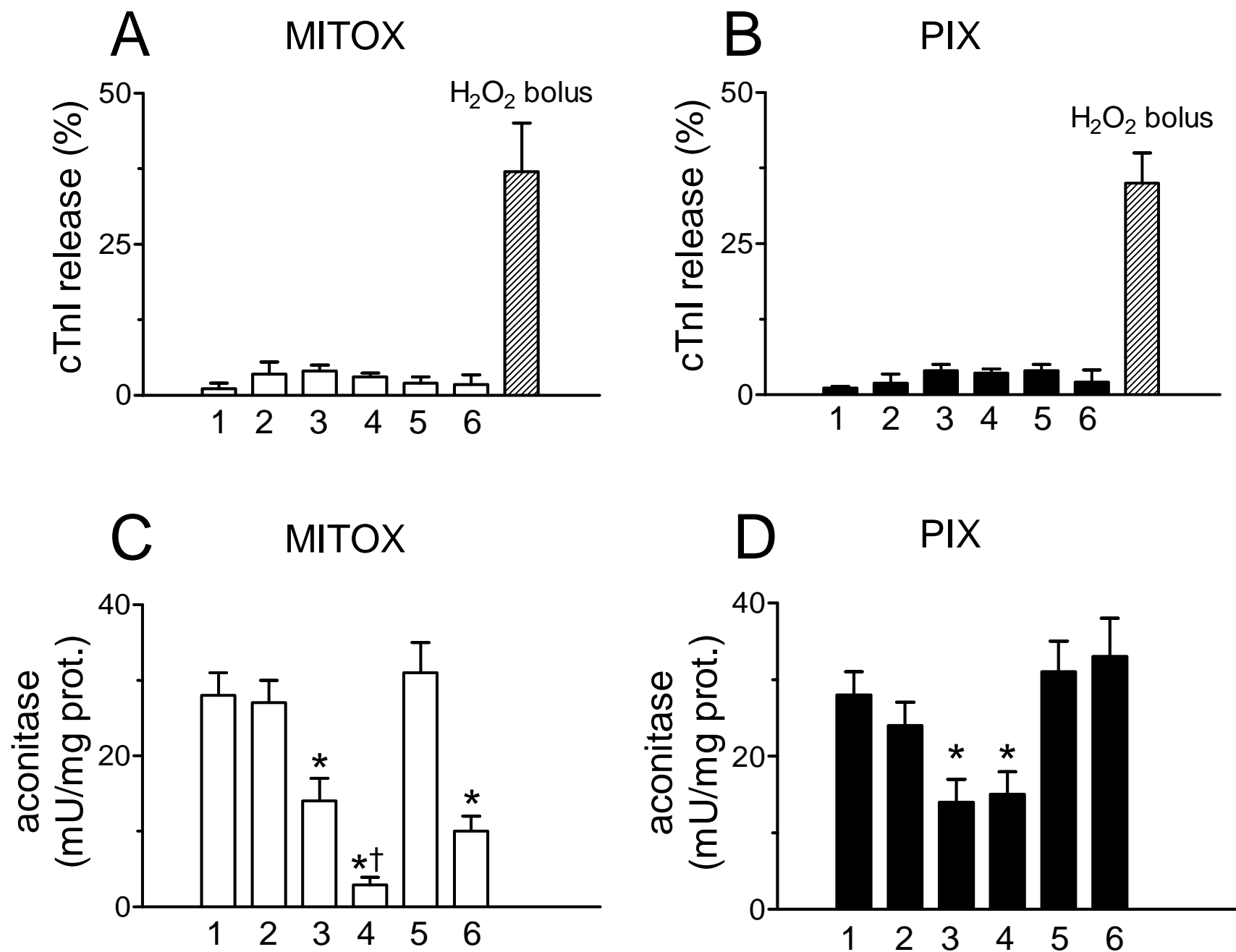| metabolite	[M-H]$^+$	oxidized residues	degree of oxidation
A	475.5	diquinone-quinoxaline-peroxyl	++++++
B	441.5	diquinone-peroxyl	+++++
C	477.5	quinoxaline-peroxyl	++++
D	443.5	quinoxaline	+++
E	443.5	diquinone	++
F	501.5	carboxyl	+

Figure 5

Figure 6

Figure 7

Figure 8

Figure 9